DEVELOPMENT OF A VISUALIZATION TECHNIQUE OF PROTON CONCENTRATION IN EXTENDED NANOSPACE CHANNEL USING STIMULATED EMISSION DEPLETION MICROSCOPY

Y. Kazoe,[*] K. Mawatari, Y. Sugii and T. Kitamori
Department of Applied Chemistry, The University of Tokyo, JAPAN

ABSTRACT

Ion behavior confined in extended nanospace (10^1–10^3 nm) is important to develop novel miniaturized systems for biochemical analysis and further applications. The present study developed a measurement technique of ion distribution in nanochannel using stimulated emission depletion microscopy to achieve a spatial resolution of 87 nm. Fluorescein was used for ratiometric measurement of pH by two-excitation wavelengths. The proton distribution in a 2D nanochannel of 410 nm width and 405 nm depth was firstly measured at an uncertainty of pH 0.05, which was strongly related to the electric double layer. This technique will greatly contribute to establish nanofluidics and nanochemistry.

KEYWORDS: Fluorescence, Stimulated emission depletion, Extended nanochannel, Proton

INTRODUCTION

Recently, miniaturized flow systems are downscaling to extended nanoscale (10^1–10^3 nm) for development of more efficient and novel applications of chemical analysis and synthesis. This scale is comparable to the scale of electric double layer (EDL), i.e., the ion layer formed by the surface charge, and specific liquid properties are induced [1, 2]. Although many researchers have focused on the ion behavior in the nanoscale, which is critical to fluid dynamics and electrokinetics [3], direct visualization method has not been realized owing to its extremely small size. On the other hand, several methods of super resolution microscopy of spatial resolution over the optical diffraction limit have been recently reported [4]. Therefore, this study developed a technique to measure the distribution of proton concentration in nanochannels, based on pH-sensitive fluorescent dye and stimulated emission depletion (STED) microscopy.

EXPERIMENTAL

A 8.6×10^{-6} mol/L fluorescein ($C_{20}H_{12}O_5$) was used as a fluorescent pH probe and dissolved into electrolyte solutions. For the pH measurements in nanochannels, three kinds of electrolyte solution of different thickness of the electric double layer, i.e., the Debye length λ_D, deionized water ($\lambda_D = 311$ nm), potassium chloride (KCl) 10^{-4} mol/L ($\lambda_D = 30$ nm) and KCl 10^{-2} mol/L ($\lambda_D = 3$ nm) were prepared.

Figure 1 illustrates an experimental apparatus. Fluorescence excited by an Ar-ion laser at peripheral region of the Gaussian intensity at a focal spot was switched off by a STED laser of 592 nm with a doughnut shape [4]. Hence only the fluorescence emitted from the molecules in the doughnuts hole of 10−100 nm was detected by an avalanche photo diode through an objective lens, the dichroic mirrors, a confocal pinhole, and an emission filter passing wavelengths of 500−550 nm. The image scanning at an interval of 33.7 nm was conducted by galvanometer mirrors. The spatial resolution in the measurement plane was 87 nm, which was evaluated by imaging fluorescent nanoparticles stuck on the glass surface [5]. The depth-wise resolution dependent on the principle of confocal microscopy was calculated to be 655 nm [6].

Figure 2(a) shows a schematic of pressure driven flow system for nanochannels. The fabrication of microchip containing nanochannels and microchannels for the sample injection has been described previously [7]. Two types of rectangular nanochannels of a same depth were fabricated on a fused-silica plate: two-dimensional (2D) nanochannel of 410 nm width and 405 nm depth and one-dimensional (1D) nanochannel of 10 μm width and 405 nm depth as illustrated in Figure 2(b). The channels were sealed with another fused silica plate of a 0.17 mm thickness by thermal fusion bonding. The sample solution was driven and injected into the nanochannels by an air pressure of 0.4 MPa.

RESULTS AND DISCUSSION

For the pH measurements using fluorescence, calibration was conducted to obtain a relationship between the pH of buffer solution and the fluorescent intensity emitted from fluorescein molecules. Fluorescein changes its chemical structure as ion and the fluorescent intensity depending on the pH of liquid. However, nonuniform distribution of fluorescein ions due to the wall electrostatic potential in nanochannel causes significant errors. Therefore, the measurement of pH in nanochannels was established based on ratiometric imaging using two excitation wavelengths. The fluorescence by 488 nm excitation has strong pH dependency while that by 458 nm excitation is almost independent [8]. A fused-silica microchannel was used for the calibration experiments in stable pH conditions without wall effects. A calibration curve was obtained from the ratio of fluorescent intensities by the 488 nm and 458 nm excitations (Figure 3). The fluorescent intensity ratio varies with the pH 3.0−7.5,
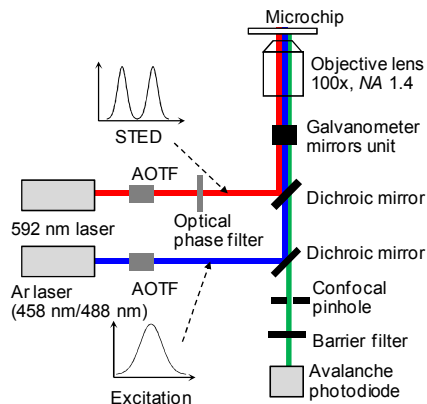
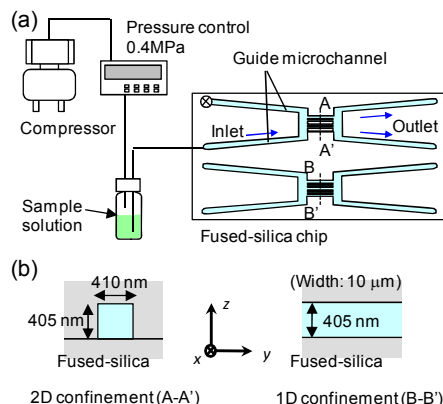Figure 1: Schematic of (a) measurement system and (b) fluorescence excitation with STED.

Figure 2: Schematic of (a) pressure driven control system and (b) cross-sectional views of nanochannels. 2D (A-A') and 1D nanochannels (B-B').
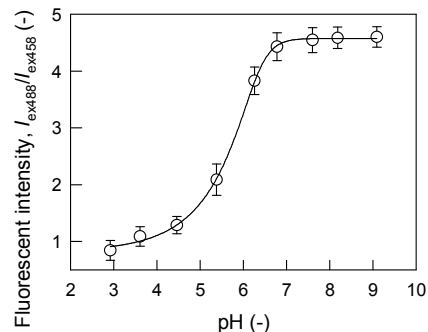

Figure 3: The ratio of fluorescent intensity by the 488 nm excitation to that by the 458 nm excitation, as function of pH.
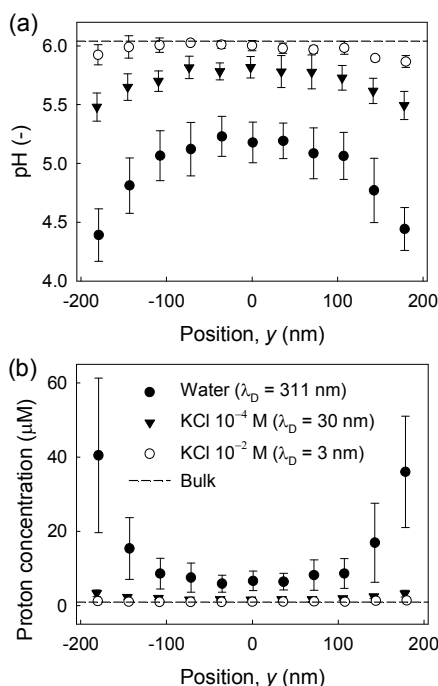

Figure 4: (a) Profiles of the pH and (b) the proton concentration in the 400 nm nanochannel for water, KCl 10^{-4} mol/L and KCl 10^{-2} mol/L, compared to the bulk pH measured in the microchannel.
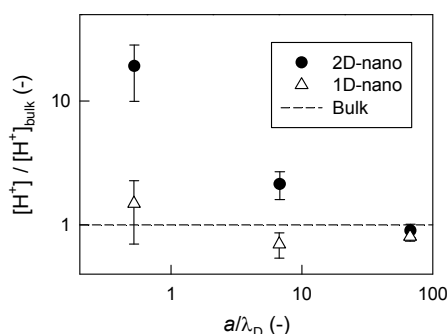

Figure 5: Ratio of the average proton concentration in the nanochannel to that of the bulk as function of the ratio of the channel radius to the Debye length, a/λ_D.

and this pH range is suitable for the measurement of the pH of aqueous solutions. These results suggest that the measurement using fluorescent indicator molecules are also applicable for the STED microscopy.

By using the calibration curve, the pH in the 400 nm nanochannels were measured. The nanochannels were imaged from a bottom-wall side in Figure 2(b) at a scanning rate of 20 μs/point for 17.3 μm × 2.2 μm (512 × 64 points). The fluorescent intensities were averaged over the *x*-direction to increase the S/N to 15.6. Then the calibration curve was applied to obtain the pH profile in the *y*-direction. The measurement uncertainty in 95% confidence level was pH 0.05.

Figure 4(a) and 4(b) show *y*-direction profiles of the pH and the proton concentration in the 400 nm 2D nanochannel, respectively. The results were compared to the bulk value of pH 6.04±0.12 (0.93±0.24 × 10^{-6} mol/L) measured in the microchannel, plotted as a dash line. When the water was flown through the nanochannel, whole region of the channel is filled by the overlapped electric double layers formed by protons to cancel the negative charge of glass surface, and the pH is lower than the bulk with the difference of pH 1−2. The concentration profile is significantly nonuniform. For the case of KCl 10^{-4} mol/L with λ_D = 30 nm, the pH is still lower than the bulk but the maximum difference is approximately pH 0.5 since the double layer is mainly formed by potassium ions (K^+). In contrast, when the KCl 10^{-2} mol/L was injected into the channel, the result shows approximately similar pH to the bulk and the uniform concentration profile since the double layer of λ_D = 3 nm is thin and negligible compared to the channel size. These results for proton concentration in the nanochannel, which were firstly observed by experiments, suggest that the ions distribute in the channel to cancel the wall charge strongly depending on the Debye length and form the electric double layer, as expected in the classical theory.

In the classical theory, colloid and fluid dynamics have been described using a ratio of the channel radius to the Debye length, a/λ_D, showing how much the double layer fills the channel [1]. Hence the results were evaluated using a/λ_D for the 1D and 2D confinements (Figure 2(b)). A ratio of the average proton concentration in the nanochannel to that in the bulk, which indicates the proton enrichment to cancel the negative charge of the fused-silica wall, was estimated and plotted as functions

of the ratio a/λ_D, shown in Figure 5. The channel radius for the 2D confinement was calculated from a hydraulic diameter of 407 nm, while that for the 1D confinement was 405 nm. The results show excess protons in the 2D nanochannel than the 1D, especially when the double layers are overlapped in the channel ($a/\lambda_D < 1$). For the 1D confinement, such the proton enrichment becomes obvious only at the double layer overlap. When the double layer is negligible compared to the channel size, both the proton concentrations in the 1D and 2D nanochannels show similar value to the bulk.

The results shown in Figure 5 indicate a specific proton transfer in the 2D nano-confinement of dilute electrolyte solution of the thick double layer. The surface to volume ratio of the 2D nanochannel with the confinement by four walls is twice of that of the 1D nanochannel by two walls. In the classical theory, since the total charge density of the channel is simply dependent on the surface to volume ratio, the proton concentration in the 2D nanochannel to cancel the wall charge is expected to be simply twice higher than the 1D nanochannel. However, contrary to this expectation, the result shows the proton concentrations in the 2D nanochannel 12.8 times and 3.1 times higher than those in the 1D nanochannel at $a/\lambda_D = 0.65$ and 6.7, respectively. Therefore, it is considered that the 2D nano-confinement enhances the proton dissociation from the silanol group at the fused-silica surface, when the double layer is comparable to the space size.

CONCLUSION

A novel fluorescence-based visualization technique of ion concentration in extended nanochannel was developed for the first time. The technique was based on the STED microscopy, which enables nanometer-order spatial resolution over the optical diffraction limit. Fluorescein was used as a probe for the pH measurement using the ratio of fluorescent intensities by 488 nm and 458 nm excitations. The calibration curve between the pH of liquid and the fluorescent intensity ratio was successfully obtained, suggesting that measurements using fluorescent indicator are available even for the STED microscopy. The profile of proton concentration in a 400 nm 2D nanochannel was firstly measured at an uncertainty in 95% confidence level of pH 0.05. The results show excess protons distribute in nanochannel to cancel negative charge of fused-silica, strongly related to the electric double layer thickness. However, the average proton concentration in the 2D nanochannel was much higher than that expected by classical theory based on the surface to volume ratio, compared to the 1D nanochannel. This suggests that the proton dissociation from the silanol group at the fused-silica surface can be enhanced by the 2D confinement in extended nanospace, for the thick double layer comparable to the space size.

REFERENCES

[1] R. F. Probstein, Physicochemical Hydrodynamics, John Wiley & Sons, New York, (1994).

[2] T. Tsukahara, K. Mawatari and T. Kitamori, "Integrated Extended-Nano Chemical Systems on a Chip," *Chem. Soc. Rev.*, vol. 39, pp. 1000-1013, (2010).

[3] F. Baldessari and J. G. Santiago, "Electrokinetics in Nanochannels Part I. Electric Double Layer Overlap and Channel-to-Well Equilibrium," *Journal of Colloid Interface Sci.*, vol. 325, pp. 526-538, (2008).

[4] S. W. Hell, "Toward Fluorescence Nanoscopy," *Nature Biotech.*, vol. 21, pp. 1347-1355, (2003).

[5] Y. Kazoe, K. Mawatari, Y. Sugii and T. Kitamori, "Development of measurement technique for ion concentration in extended nanochannel by super resolution-laser induced fluorescence," *Anal. Chem.*, submitted.

[6] J. S. Park, C. K. Choi, K. D. Kihm, "Optically sliced micro-PIV using confocal laser scanning microscopy," *Exp. Fluids*, vol. 37, pp. 105-119, (2004).

[7] T. Tsukahara, K. Mawatari, A. Hibara and T. Kitamori, "Development of a pressure-driven nanofluidic control system and its application to an enzymatic reaction," *Anal. Bioanal. Chem.*, vol. 391, pp. 2745-2752, (2008).

[8] R. Sjöback, J. Nygren and M. Kubista, "Absorption and fluorescence properties of fluorescein," *Spectrochimica Acta Part A*, vol. 51, pp. L7-L21, (1995).

CONTACT

*Y. Kazoe, tel: +81-3-5841-7231; kazoe@icl.t.u-tokyo.ac.jp